The Effect of Processing Conditions on the Fracture Behavior of Syndiotactic Polystyrene Films

S. WU,[1] R. A. BUBECK,[2] and C. J. CARRIERE[3,*]

The Dow Chemical Company, [1]North American Analytical Sciences Laboratory, B-1470B, Freeport, Texas 77459, [2]North American Analytical Sciences Laboratory, 1897 Bldg., Midland, Michigan 48674, and [3]Central Research & Development, 1702 Bldg, Midland, Michigan 48674

SYNOPSIS

A fracture behavior map for syndiotactic polystyrene (sPS) film as a function of annealing temperature and the extension ratio has been developed. The fracture initiation and propagation processes of the film were characterized by a specialized video-based real-time thin-film fracture technique. An unusual layered complex deformation mechanism has been observed for the films fabricated at high extension ratios. This mechanism enhances the resistance to crack growth in sPS films. © 1996 John Wiley & Sons, Inc.

INTRODUCTION

Fracture toughness tests for polymeric films has recently been reported by several authors.[1-3] Because of the complication of the mixed plane stress/plane strain loading in thin films, the applicability of plane strain toughness parameters such as the critical stress intensity factor and the energy release rate as applied to thin polymer films has been discussed by various authors.[4,5] The toughness of films has to be related to the observed process zones (defined as the damage area) near the crack tip during crack initiation. To account for the effect of the process zone on the toughness, the deformation mechanisms have to be characterized for each material, and the relationship between those fracture mechanisms and the toughness of the materials has to be established. This leads to difficulties in interpreting the toughness of polymeric films, which involve multiple deformation mechanisms.

Material properties, especially the correlation between processing and fracture behavior, are primary concerns. The fracture behavior and toughness of the film is important because the material must be able to withstand the stresses encountered during fabrication as well as during use. Depending on processing history, the deformation mechanisms of the films include small-scale yielding, large-scale yielding (strain hardening), and/or crazing. Because it is very difficult to interpret the toughness of these films when there are various deformation mechanisms involved, this work focuses primarily on direct observation of the effect of processing conditions on the resulting deformation mechanisms.

In this study, both fracture initiation and propagation were characterized by a specialized video-based real-time thin-film fracture technique. A fracture behavior map at crack initiation has been developed that provides valuable information on the effect of processing on the properties of syndiotactic polystyrene (sPS) films. A complex deformation mechanism has been observed and characterized for sPS film. This new complex mode, which contains a layered structure inside the process zone, increases the resistance of material to crack propagation.

EXPERIMENTAL

Materials

The sPS materials used in this study were obtained from The Dow Chemical Company. The materials were obtained as extruded sheets approximately 30 cm wide by 60 cm long by 0.1 cm thick. The starting material had a nominal weight average molecular

* To whom correspondence should be addressed.

Journal of Applied Polymer Science, Vol. 62, 1483–1490 (1996)
 CCC 0021-8995/96/091483-08

weight of 350 kg/mol. All the materials were used as received.

Sample Film Preparation

The sPS sheets were stretched biaxially at 110°C to extension ratios of 1.5×, 2×, 2.5×, and 3× using an Iwamoto biaxial stretcher. Prior to stretching the sheets were allowed to equilibrate in the Iwamoto for 1.5 min. All the films were fabricated at an extension rate of 10 mm/s. Although the films were stretched to the same extension ratio in both directions, the total extension history in each direction were somewhat different because the original sheet was made by extrusion. The films are, therefore, expected to possess some anisotropy.

Annealing

sPS can be crystallized in different forms.[6,7] Second-stage thermally induced crystallization has recently been reported in sPS materials that have undergone rapid cooling.[8] The results show that the growth of the ordered structure occurs in two stages: (1) a fast primary stage, followed by (2) a slower secondary process. The primary stage is temperature dependent and proceeds at an increasing rate at elevated annealing temperatures. The annealing times and temperatures for the materials reported in this study were 20 min at 120°C, 5 min at 160°C, 1 min at 200°C, or 30 s at 240°C. To prevent distortion of the film specimen during annealing, the sample was constrained using a steel frame. The constrained sample was then placed in a Fischer Isotemp™ 838F air-circulating oven that had been preset to the desired temperature. After the annealing time had been reached the sample was extracted from the oven and allowed to cool to room temperature before removal from the frame.

Fracture Specimen Preparation and Notch Sensitivity

Single-edge notch (SEN) specimens of sPS were prepared from the biaxially oriented films by first cutting the specimens into 127-mm long and 9-mm wide strips with a surgical blade. Because the material properties of the film are not completely isotropic, all the samples were cut along the original extrusion direction. A small cutting machine was utilized to cut the crack to a specified crack length. Of the different cutting methods tried for sPS films, including surgical blades and scissors, the cutting machine method tended to minimize damage, or crazing, near the crack tip. The other methods tended to cause crack branching, excessive crazing, or kinking, especially near the crack tip.

Fracture Experiments

A schematic of the experimental setup is illustrated in Figure 1. The investigations were conducted using an Instron 8800 servo-hydraulic testing frame equipped with self-tightening grips and operating under Instron Series IX software control. All the experiments were performed at room temperature at a deformation rate of 1.27 mm/min. Typically, 15 to 20 specimens were evaluated for each condition.

The crack tip region in the specimen was videotaped using a microscope mounted on a traveling stage. The stage allowed the developing crack and associated deformation zone to be followed easily. Stress levels were superimposed onto the microscope video image by attaching an external computer equipped with a data acquisition board to the load cell. The stress values displayed on the computer screen were inserted into a corner of the video image of the specimen by means of a video camera and mixer. Stress values at crack initiation then can be determined by analyzing the video tape in slow motion. The deformation process zone evolution as well as the crack initiation and propogation process can be observed and later quantified by viewing the video tape.

Quantification of the fracture strength of the materials investigated in this work were characterized using the critical energy release rate, J_{1c}, and the energy release rate to break, J^*. These quantities

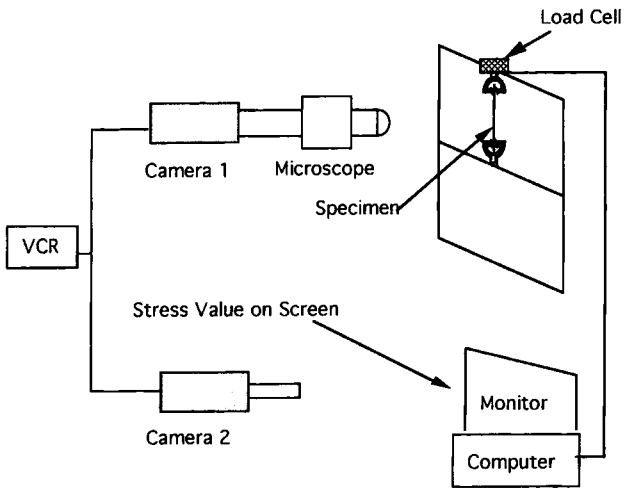

Figure 1 Schematic of the thin-film fracture toughness apparatus with a video-based data acquisition system.

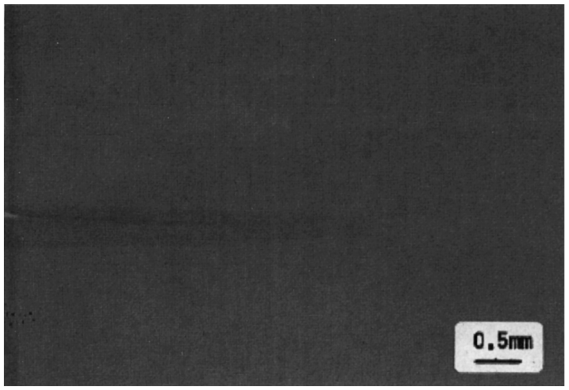

Figure 2 Micrograph of a brittle fracture of sPS film (extension ratio 1×, heat setting temperature 240°C, film thickness of 0.24 mm). Micrograph taken perpendicular to the film surface.

represent the lower and upper limits of the material's toughness. These parameters also can be used to represent the materials resistance to crack initiation and crack growth. The critical energy release rate at crack initiation is defined as[9]

$$J_{1c} = \frac{\sigma_c^2 \pi L}{E} f^2(L/W) \tag{1}$$

where σ_c is the critical stress at crack initiation, L is the crack length, $f\left(\frac{L}{W}\right)$ is the geometry factor, W is the specimen width, and E is the elastic Young's modulus. It should be mentioned that although eq. (1) is identical to that quoted typically for the elastic energy release rate G_{1c}, J_{1c} is not identical to G_{1c}, because the critical stress at crack initiation is not the same as in the formula for G_{1c}. In the study reported here, σ_c was obtained as the critical stress at crack initiation by reviewing the crack initiation process from the video tape. Only for a linear elastic material will J_{1c} equal G_{1c}.

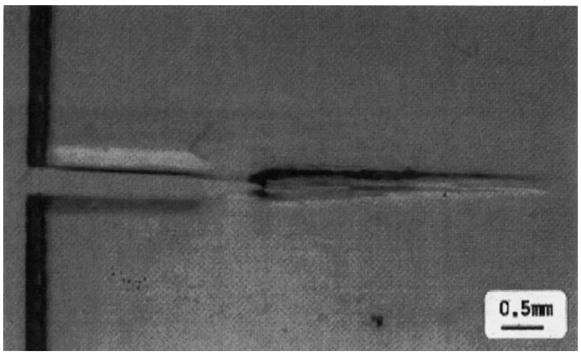

Figure 4 Micrograph of a mixed craze and yielding zone near the crack tip of sPS film (extension ratio 1.5, heat setting temperature 120°C, thickness 0.14 mm). Micrograph taken perpendicular to the film surface.

The energy release rate to break, J^*, is defined as:

$$J^* = \frac{\Delta\Pi}{(W - L)t}, \tag{2}$$

where $\Delta\Pi$ is the total energy release to break the specimen (which is typically taken as the area under the stress–strain curve) and t is the thickness of specimen. In the limit, a linear elastic material will have a value for J_{1c} that may coincide with the value of J^* if one ignores the effect of machine compliance. As soon as there are nonelastic deformations during crack initiation or growth, however, J^* is typically larger than.

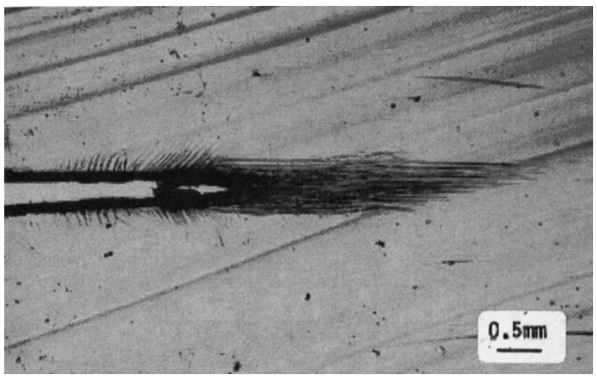

Figure 3 Micrograph of a craze zone near the crack tip of sPS film (extension ratio 2×, heat setting temperature 200°C, film thickness 0.20 mm).

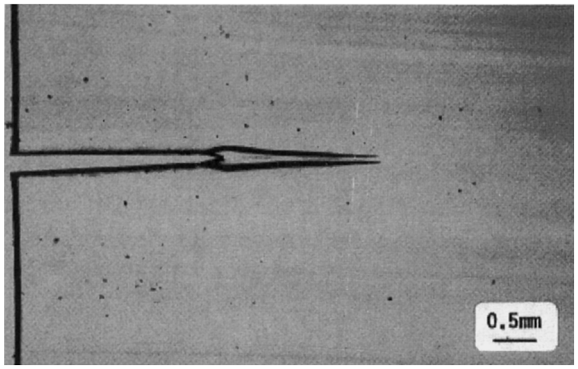

Figure 5 Micrograph of a yielding zone near the crack tip of sPS film (extension ratio 2.5, without heat setting, film thickness 0.20 mm). Micrograph taken perpendicular to the film surface.

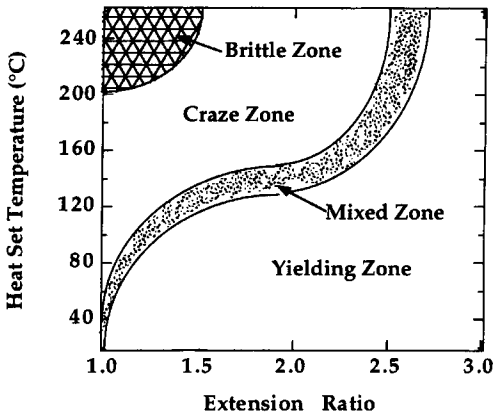

Figure 6 The fracture behavior map for sPS films.

Tensile Property Evaluation

The elastic Young's modulus and yield or break strength of the various sPS films were evaluated using an Instron 8800 servo-hydraulic test frame equipped with self-tightening grips operating under Instron Series IX software control. All the experiments were performed at room temperature without an extensometer at a deformation rate of 1.27 mm/min. Typically, 5 to 10 test specimens were run for each condition investigated.

OBSERVATION AND DISCUSSION

Fracture Behavior at Crack Initiation

In the course of this study various fracture mechanisms have been observed for sPS films as functions of extension ratio and annealing conditions. A classical brittle crack in sPS film, illustrated in Figure 2, is observed when the annealing temperature is above 200°C and the extension ratio is less than 1.5. In this case, the crack became unstable soon after crack initiation. If the annealing temperature is lowered, or the extension ratio is increased, a craze array can be produced near the crack tip prior to the crack reaching instability. This case is illustrated in Figure 3. Crazing and yielding inside the deformation process zone is observed for decreasing annealing temperature or increasing extension ratio (Fig. 4). Quasi-static crack growth after crack initiation has been observed in this case. A yielding process zone is illustrated in Figure 5, which is observed with a low annealing temperature and high extension ratio. Because of the irreversible deformation inside the process zone, a slow crack growth after initiation was observed.

A fracture behavior map has been developed by combining all of the observations of deformation behavior at crack initiation as a function of annealing condition and extension ratio. The fracture behavior map is illustrated in Figure 6. In this map, four regions have been distinguished by the fracture behavior discussed above at crack initiation, i.e., brittle zone, craze zone, mixed zone, and yielding zone. It should be emphasized that the boundary of these regions are only approximate, due to the limited data available. The toughness of sPS films in the same fracture mechanism region are not necessarily identical because the toughness not only

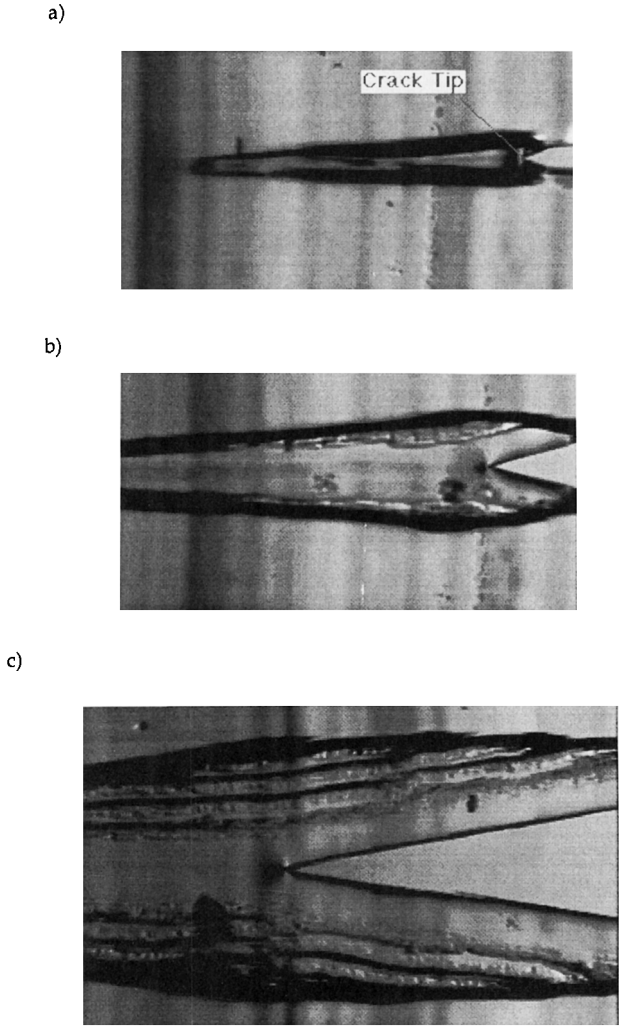

Figure 7 Micrographs (40×) of the process zone evolution with a complex deformation mechanism (extension ratio 2×, without heat setting). (a) Process zone at crack initiation; (b) the internal deformation appears after crack initiation; (c) the layer structure inside the process zone. Micrographs taken perpendicular to the film surface.

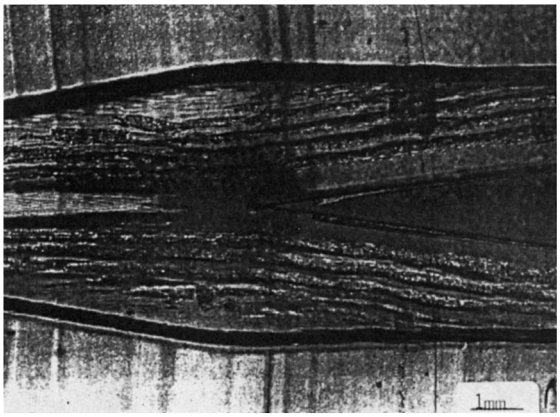

Figure 8 The optical micrograph of process zone with a layered structure (extension ratio 2×, without annealing). Micrograph taken perpendicular to the film surface.

depends upon the fracture mechanisms, but also upon the size and shape of the process zone.

Complex Deformation Mechanism

A complex deformation mechanism has been observed for sPS films with extension ratios of 2× in the absence of annealing. The crack initiation and growth processes are shown by a series of micrographs in Figure 7. After crack initiation, a layer structure appears near the boundary of the process zone. As the crack advances, more layers are developed with nearly constant distance between them [about 0.1 mm, as shown in Fig. 7(c)]. In the center of the process zone, the distance between the upper and lower layers also remains constant. The layer structures inside the process zone has been investigated using optical microscopy. The optical micrographs of the layer structure are shown in Figure 8, where the dark lines are the boundary of the process zone. The layered structures are induced by light reflection from regions of the internal deformation. Investigations using a SEM, however, found that the layer structures inside the process zone are mainly internal microcracking and voids where formation is enhanced by the high in-plane orientation much as very high orientation polymer fibers can fibrilate with the separations running parallel to the applied tensile stress. SEM micrographs of the cross-section of the process zone are exhibited in Figure 9.

Toughness Evaluation of sPS Films

Efforts were concentrated in this investigation on two lines in the fracture behavior map: (1) a constant extension ratio of 1.5× with variable heat setting conditions, and (2) variable extension ratios without any heat setting. First, uniaxial tensile tests were performed to check the effect of processing condi-

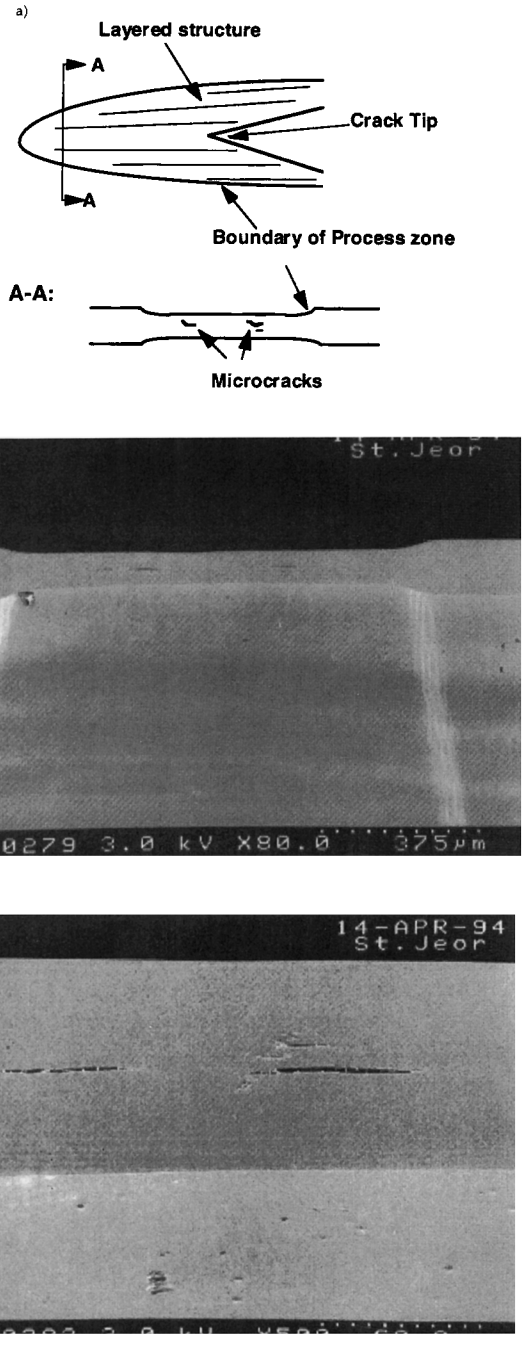

Figure 9 Analysis of deformation inside the process zone of a thin-film sample of sPS processed with an extension ratio of 2× without annealing: (a) the sketch of the process zone and cross-section; (b) SEM micrograph of internal deformation of the tip of layer; (c) SEM micrograph of internal crazing and voids.

Table I Summary of the Effects of Annealing Temperature and Extension Ratio on the Tensile and Fracture Properties of sPS Films

Extension Ratio	Annealing Temperature (°C)	Modulus (GPa)	Maximum Strain	J_{1C} (kN/m)	J^* (kN/m)
1.0	None	2.6 ± 0.2	2.0 ± 0.2	4.41 ± 0.69	16.44 ± 6.56
1.5	None	2.45 ± 0.15	10 ± 0.1	5.39 ± 1.40	25.36 ± 7.62
2.0	None	2.7 ± 0.1	11 ± 4	5.28 ± 1.13	42.89 ± 7.31
2.5	None	3.0 ± 0.1	35 ± 4	4.48 ± 1.36	25.92 ± 8.18
3.0	None	3.4 ± 0.2	40 ± 5	1.31 ± 0.19	17.20 ± 7.30
1.5	120	2.5 ± 0.3	6.5 ± 1.5	4.98 ± 1.02	18.46 ± 5.64
1.5	160	2.7 ± 0.1	3.0 ± 0.1	4.16 ± 0.35	15.32 ± 7.18
1.5	200	3.1 ± 0.2	2.0 ± 0.5	1.11 ± 0.79	5.09 ± 2.31
1.5	240	3.1 ± 0.2	1.6 ± 0.2	0.21 ± 0.02	0.83 ± .09

tions on the mechanical properties according to ASTM standards (ASTM D412 type C) and then the fracture tests were performed to check the effect of processing conditions on the fracture toughness of sPS films.

The Effect of Heat Setting

The mechanical properties studies were performed for sPS films subjected to an extension ratio 1.5× with heat setting temperatures at room temperature (or no heat setting), 120, 160, 200, and 240°C. The results for Young's modulus and maximum strain are summarized in Table I. Before the specimen fractured, shear bands were observed for the cases of (1) specimens not subjected to heat setting, or (2) specimens subjected to a heat setting temperature of 120°C. Crazes were observed for specimens heat set at 160°C. For specimens with heat setting at a temperature of 200 or 240°C, fracture was observed to occur in a brittle fashion.

The effect of heat setting conditions on the fracture strengths of the sPS films subjected to an extension ratio of 1.5× are illustrated in Figure 10 and summarized in Table I. It should be noted that the critical energy release rate at crack initiation and energy release rate to break are both a function of crack length. The energy release rate to break increases as the ligament of the specimen (or the crack increment) is increased. This is not the J-R curve in the conventional sense, but it does show the dependence of energy release rate on the crack length.

The Effect of Extension Ratio

The mechanical properties were measured for non-heat set films with extension ratios of 1×, 1.5×, 2×, 2.5×, and 3×. The results for the maximum strain and Young's modulus are summarized in Table I. For the case of specimens with an extension ratio of 1×, crazes were formed before the specimen fractured. Shear bands were observed prior to fracture for the case of specimens with an extension ratio of 1.5×, while shear bands were observed to form at first followed by uniform yielding for the cases of extension ratios of 2× and 2.5×. For specimens fabricated with an extension ratio 3×, fracture occurred after specimen yielding.

The effects of extension ratio on the critical energy release rate at crack initiation and energy release rate to break for sPS films that were not subjected to annealing temperatures are shown in Figure 11 and summarized in Table 1. It is interesting to note that the energy release rate to break data display a marked maximum at an extension ratio of 2×.

Complex Deformation Mechanism and Film Toughness

The maximum strain obtained from a stress–strain curve for single-edge notch specimens reflect indirectly the crack propagation process. Brittle samples will have a low value for the maximum strain, while ductile samples will possess a relatively high value provided the test conditions and sample geometry are fixed. Stress–strain curves for sPS thin notched films processed with various extension ratios, without annealing, are illustrated in Figure 12. The largest break strain is obtained with the film processed using an extension ratio of 2×. It is reasonable to assume that the unusual layered deformation mechanism shown in Figure 7 is responsible. The internal voids or crazes shown in Figure 8 are most likely the result of localized constraints associated with the crystal

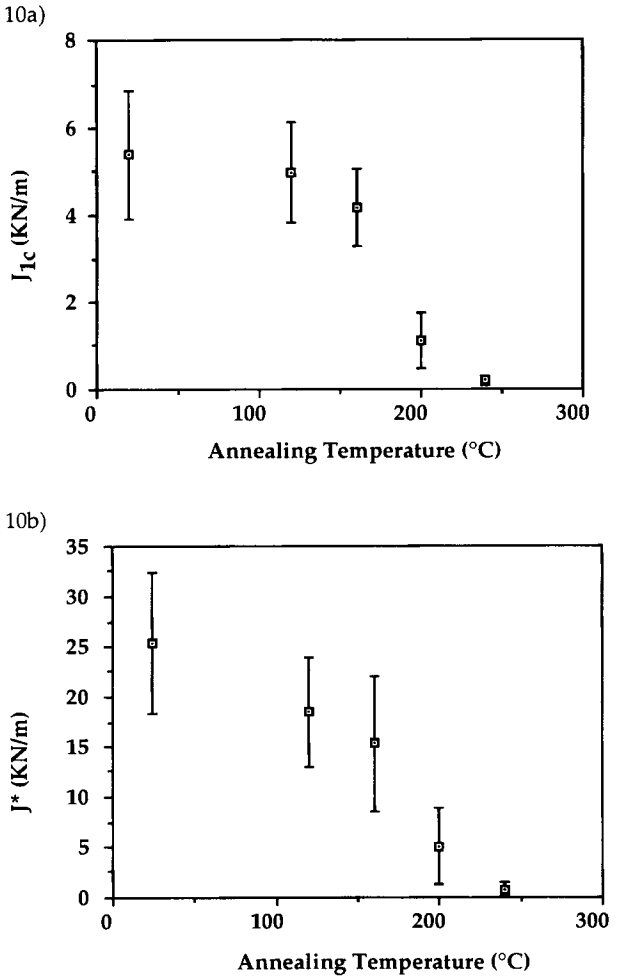

Figure 10 The effect of annealing temperature on the (a) critical energy release rate, J_{1c}, or (b) the energy release rate to break, J^*, for sPS films prepared with an extension ratio of 1.5×.

orientation. This mechanism appears to contribute to the increased toughness of the film. It is well known that any irreversible deformations ahead of the crack tip will shield the crack, thus reducing the stress intensity near the crack tip. The difference is that this toughening mechanism can be achieved by controlling the processing condition of sPS films. Although requiring further investigation, the enhanced toughness is presumed to be related to understandable factors associated with the planar orientation and microstructure of the film.

It should be emphasized that the thickness of the films are not uniform, and are correspondingly thinner for materials processed with higher extension ratios. The competition between crazing and shear yielding on the fracture toughness has been discussed by many authors, including the transition from plane strain fracture to plain stress fracture.[5,10-12] According to the ASTM standards for evaluation of J_{1c},[13,14] the thickness of the specimen must be greater than or equal to $25 \frac{G_{1c}}{\sigma_y}$, where σ_y is the yielding stress of the material. For the materials discussed herein, the estimated required transition thickness has been estimated to be about 1.1 mm. Because all of the samples evaluated had thickness much smaller than 1 mm (samples thickness varied from approximately 0.2 to 0.02 mm), all of the tests were, principally, conducted under plane stress fracture conditions. Thus, it is unlikely the brittle-ductile transition observed in this study was induced principally by thickness variation, but rather by

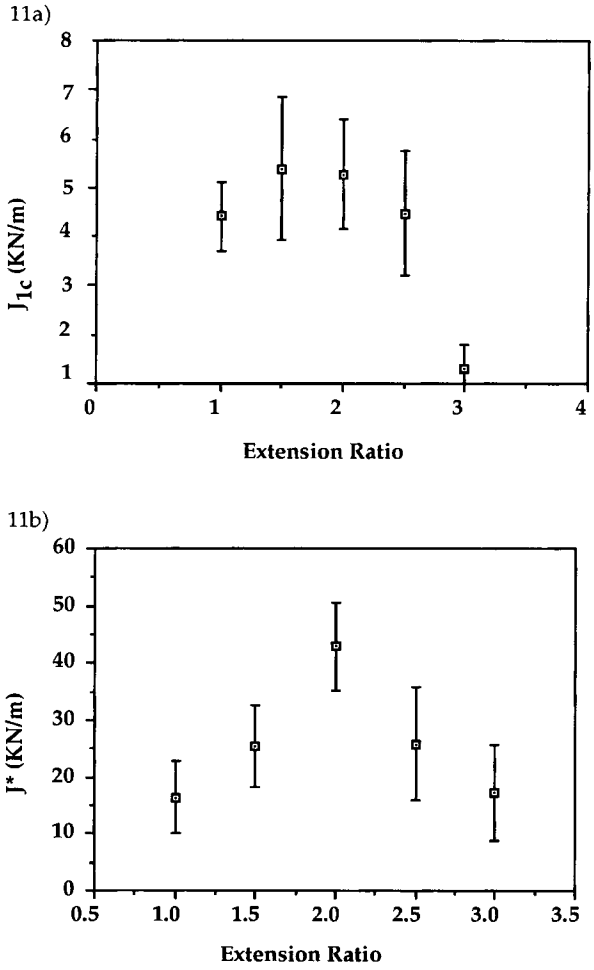

Figure 11 The effect of extension ratio on the (a) critical energy release rate, J_{1c}, or (b) the energy release rate to break, J^*, for sPS films that had not been subjected to annealing temperatures.

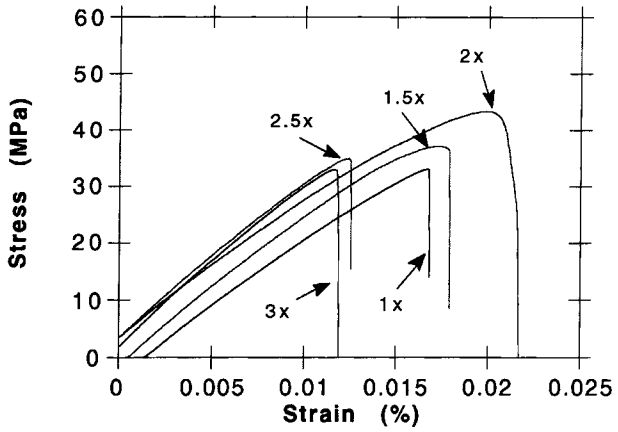

Figure 12 Engineering stress–strain curves of single-edge notch thin-film sPS samples. The specimens were produced without annealing. The curves were generated at room temperature.

morphological changes associated with the annealing process.

SUMMARY

An unusual layered complex-mode deformation mechanism has been observed for highly oriented sPS films. The layered structure was formed by microcracking along the loading direction in the plane of the film. This mechanism enhances the resistance to crack growth in this material.

A fracture behavior map of sPS film as a function of annealing temperature and extension ratio has been developed. This map provides valuable information about the effect of processing conditions on the deformation and fracture behavior of sPS films. These maps can serve as a useful tool for the consideration of sPS films for various applications, and for film fabricators who need to post process sPS films for final applications.

The authors would like to thank our colleagues Var St. Jeor for the scanning electron microscopy analysis, Yi-Bin Huang and Mark Sonnenschein for supplying and fabricating the sPS sheet.

REFERENCES

1. J. A. Hinckley and S. L. Mings, *Polymer,* **31,** 75 (1990).
2. A. H. Tsou, J. S. Hord, G. D. Smith, and R. W. Schrader, *Polymer,* **33,** 2970 (1992).
3. S. Hashemi, *J. Mater. Sci.,* **28,** 6178 (1993).
4. J. M. Hodgkinson and J. G. Williams, *J. Mater. Sci.,* **16,** 50 (1981).
5. O. F. Yap, Y. W. Mai, and B. Cotterell, *J. Mater. Sci.,* **18** 657 (1983).
6. N. Ishiara, T. Seimiya, N. Kuramoto, and M. Uoi, *Macromolecules,* **19,** 2464 (1986).
7. O. Greis, Y. Xu, T. Asano, and J. Petermann, *Polymer,* **30,** 590 (1989).
8. F. de Candia, A. Ruvolo Filho, and V. Vittoria, *Colloid Polym. Sci.,* **269,** 650 (1991).
9. H. L. Ewalds and R. J. H. Wanhill, *Fracture Mechanics,* Edward Arnold, London, 1991, p. 145.
10. J. G. Williams, *Fracture Mechanics of Polymers,* Harwood, London, 1984, Chapt. 6, p. 123.
11. M. T. Takemori, in *Crazing in Polymers,* Vol. 2, Advances in Polymer Science, 91/92, H.-M. Kauseh, Ed., Springer Verlag, Berlin, 1990.
12. T. J. Chen, C. P. Bosnyak, and A. Chudnovsky, *J. Appl. Polym. Sci.,* **49,** 1909 (1993).
13. ASTM E813–89, ASTM Standards, 1989.
14. ASTM E1152–89, ASTM Standards, 1989.

Received April 19, 1996
Accepted May 15, 1996